Eidgenössische Technische Hochschule Zürich
Swiss Federal Institute of Technology Zurich

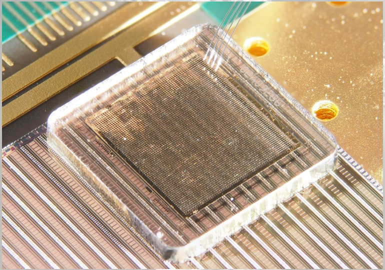

New Beam Test Results of 3D Pixel Detectors Constructed With Poly-Crystalline CVD Diamond

29th International Symposium on Lepton Photon Interactions at High Energies, Toronto, ON, Canada

Michael Reichmann on behalf of the RD42 Collaboration

8 August 2019

Table of Contents

Section 1

Motivation

Diamond as Detector Material

- innermost tracking layers $\rightarrow$ highest radiation damage $\mathcal{O}\left(\mathrm{GHz/cm^2}\right)$
- current detectors is designed to survive $\sim$12 month in High-Luminosity LHC
- $\rightarrow$ **R&D for more radiation tolerant detector designs and/or materials**

Diamond as Detector Material

- innermost tracking layers $\rightarrow$ highest radiation damage $\mathcal{O}\left(\mathrm{GHz/cm^2}\right)$
- current detectors is designed to survive ∼12 month in High-Luminosity LHC
- $\rightarrow$ **R&D for more radiation tolerant detector designs and/or materials**

Diamond as Detector Material:

- properties
  - radiation tolerant
  - isolating material
  - high charge carrier mobility
  - **smaller signal than in silicon with same thickness (large bandgap)**
  - **after $1 \cdot 10^{16}\,\mathrm{n/cm^2}$ the mean drift path in diamond larger than in silicon**

Diamond as Detector Material

- innermost tracking layers → highest radiation damage $\mathcal{O}\left(\mathrm{GHz/cm^2}\right)$
- current detectors is designed to survive ∼12 month in High-Luminosity LHC
- → **R&D for more radiation tolerant detector designs and/or materials**

Diamond as Detector Material:

- properties
  - radiation tolerant
  - isolating material
  - high charge carrier mobility
  - **smaller signal than in silicon with same thickness (large bandgap)**
  - **after $1 \cdot 10^{16}$ n/cm^2 the mean drift path in diamond larger than in silicon**

Work of RD42:

- investigate signals and radiation tolerance in various detector designs:
  - Pad Detectors → whole diamond as single cell readout
  - Pixel Detectors → diamond sensor on pixel readout chip
  - 3D Pixel Detectors → 3D diamond detector on pixel readout chip

Diamond as Detector Material

- innermost tracking layers → highest radiation damage $\mathcal{O}\left(\mathrm{GHz/cm^2}\right)$
- current detectors is designed to survive ∼12 month in High-Luminosity LHC
- → **R&D for more radiation tolerant detector designs and/or materials**

Diamond as Detector Material:

- properties
  - radiation tolerant
  - isolating material
  - high charge carrier mobility
  - **smaller signal than in silicon with same thickness (large bandgap)**
  - **after $1 \cdot 10^{16}\,\mathrm{n/cm^2}$ the mean drift path in diamond larger than in silicon**

Work of RD42:

- investigate signals and radiation tolerance in various detector designs:
  - Pad Detectors
  - Pixel Detectors
  - **3D Pixel Detectors** → this talk

RD42 Collaboration

A. Alexopoulos[3], M. Artuso[20],
F. Bachmair[24],L. Bäni[24],M. Bartosik[3], J. Beacham[13], H. Beck[23],
V. Bellini[2], V. Belyaev[12], B. Bentele[19], A. Bes[27], J-M. Brom[7],
M. Bruzzi[4], G. Chiodini[26], D. Chren[18], V. Cindro[9], G. Claus[7],
J. Collot[27], J. Cumalat[19], A. Dabrowski[3], R. D'Alessandro[4],
D. Dauvergne[27], W. de Boer[10], S. Dick[13], C. Dorfer[24],
M. Dünser[3], G. Eigen[30], V. Eremin[6], G.T. Forcolin[22],
J. Forneris[15], L. Gallin-Martel[27], M.L. Gallin-Martel[27],
K.K. Gan[13], M. Gastal[3], C. Giroletti[17], M. Goffe[7], J. Goldstein[17],
A. Golubev[8], A. Gorišek[9], E. Grigoriev[8], J. Grosse-Knetter[23],
A. Grummer[21], B. Gui[13], M. Guthoff[3], B. Hiti[9], D. Hits[24],
M. Hoeferkamp[21], T. Hofmann[3], J. Hosselet[7], J-Y. Hostachy[27],
F. Hügging[1], C. Hutton[17], J. Janssen[1], H. Kagan[13],
K. Kanxheri[28], G. Kasieczka[24], R. Kass[13], M. Kis[5],
G. Kramberger[9], S. Kuleshov[8], A. Lacoste[27], S. Lagomarsino[4],
A. Lo Giudice[15], I. López Paz[22], E. Lukosi[25], C. Maazouzi[7],
I. Mandic[9], A. Marino[19], C. Mathieu[7], M. Menichelli[28],
M. Mikuž[9], A. Morozzi[28], J. Moss[29], R. Mountain[20], A. Oh[22],
P. Olivero[15], D. Passeri[28], H. Pernegger[3], R. Perrino[26],
M. Piccini[28], F. Picollo[15], M. Pomorski[11], R. Potenza[2],
A. Quadt[23], F. Rarbi[27], A. Re[15], M. Reichmann[24], S. Roe[3],
D.A. Sanz Becerra[24], M. Scaringella[4], C.J. Schmidt[5],
E. Schioppa[3], S. Schnetzer[14], S. Sciortino[4], A. Scorzoni[28],
S. Seidel[21], L. Servoli[28], D.S. Smith[13], B. Sopko[18], V. Sopko[18],
S. Spagnolo[26], S. Spanier[25], K. Stenson[19], R. Stone[14],
B. Stugo[30], C. Sutera[2], M. Traeger[5], W. Trischuk[16],
D. Tromson[11], M. Truccato[15], C. Tuve[2], J. Velthuis[17],
S. Wagner[19], R. Wallny[24], J.C. Wang[20], J. Weingarten[23],
C. Weiss[3], N. Wermes[1], M. Yamouni[27], M. Zalieckas[30],
M. Zavrtanik[9]

117 participants

[1] Universität Bonn, Bonn, Germany
[2] INFN/University of Catania, Catania, Italy
[3] CERN, Geneva, Switzerland
[4] INFN/University of Florence, Florence, Italy
[5] GSI, Darmstadt, Germany
[6] Ioffe Institute, St. Petersburg, Russia
[7] IPHC, Strasbourg, France
[8] ITEP, Moscow, Russia
[9] Jožef Stefan Institute, Ljubljana, Slovenia
[10] Universität Karlsruhe, Karlsruhe, Germany
[11] CEA-LIST Technologies Avancees, Saclay, France
[12] MEPHI Institute, Moscow, Russia
[13] The Ohio State University, Columbus, OH, USA
[14] Rutgers University, Piscataway, NJ, USA
[15] University of Torino, Torino, Italy
[16] University of Toronto, Toronto, ON, Canada
[17] University of Bristol, Bristol, UK
[18] Czech Technical University, Prague, Czech Republic
[19] University of Colorado, Boulder, CO, USA
[20] Syracuse University, Syracuse, NY, USA
[21] University of New Mexico, Albuquerque, NM, USA
[22] University of Manchester, Manchester, UK
[23] Universität Göttingen, Göttingen, Germany
[24] ETH Zürich, Zürich, Switzerland
[25] University of Tennessee, Knoxville, TN, USA
[26] INFN-Lecce, Lecce, Italy
[27] LPSC-Grenoble, Grenoble, France
[28] INFN-Perugia, Perugia, Italy
[29] California State University, Sacramento, CA, USA
[30] University of Bergen, Bergen, Norway

30 institutes

Section 2

3D Diamond Detector

Diamond as Particle Detector

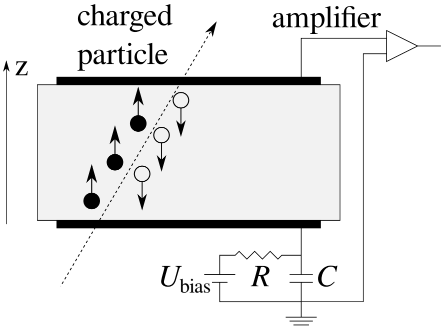

(a) Detector Schematics

(b) 15 cm ⌀ pCVD Diamond Wafer

- detectors function as ionisation chambers
- metallisation on both sides
- poly-crystals produced in large wafers

Working Principle

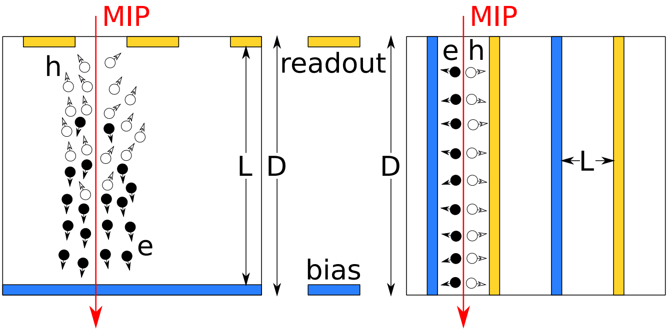

- after large radiation fluence all detectors become trap limited
- 3D = bias and readout electrode inside detector material
- same thickness D $\rightarrow$ same amount of induced charge $\rightarrow$ shorter drift distance L
- **increase collected charge in detectors with limited mean drift path (Schubweg)**
- **introduce low field regions**

Electric Field Simulation

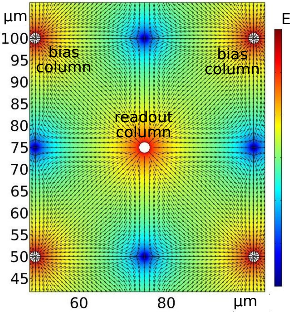

- simulation with 30 V bias voltage and periodic boundary conditions
- electric field ∼1 V/µm over a large area in the cell
- low field region in between the electrodes

Laser drilling

- "drilling" columns using 800 nm fs-LASER (Oxford)
- convert diamond into resistive mixture of carbon phases (i.a. DLC, graphite, ...)
- usage of Spatial Light Modulator (SLM) to correct for vertical aberration
- initial column yield $\sim$90 % $\rightarrow$ now $\geq$99.8 %
- initial column diameter 6 $\sim$ 10 µm $\rightarrow$ now 2.6 µm

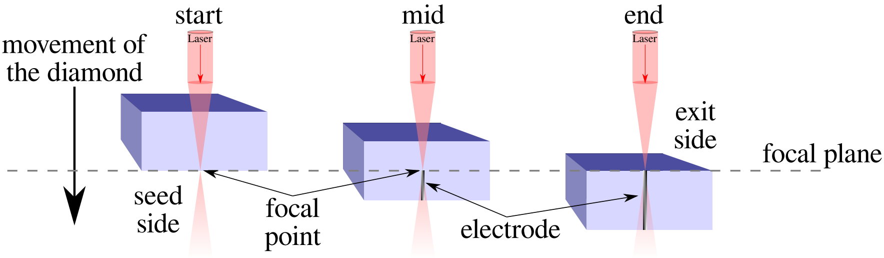

Bump Bonding

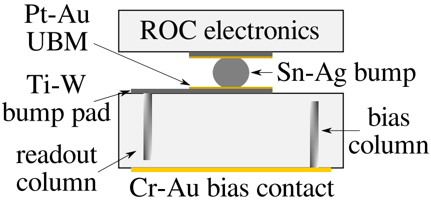

(a) Bump bond schematics

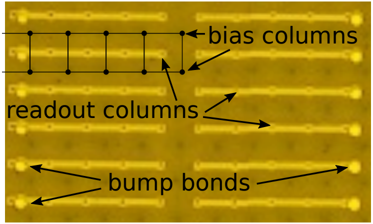

(b) 5 × 1 bump pads

- connection to bias and readout with surface metallisation
- ganging of cells to match pixel pitch of readout-chip (ROC)
- small gap (∼15 µm) to the surface

Bump Bonding

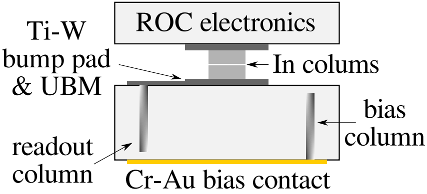

(a) Bump bond schematics

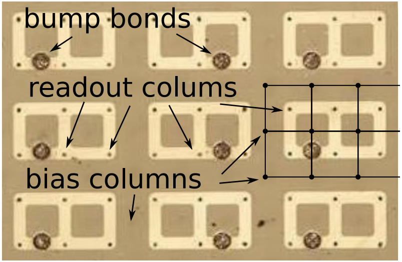

(b) 3 × 2 bump pads

- connection to bias and readout with surface metallisation
- ganging of cells to match pixel pitch of readout-chip (ROC)
- small gap (∼15 μm) to the surface

Progress in Diamond Detectors

3D Detectors - History in Diamonds:

- proved that 3D works in pCVD diamond
- scale up the number of columns per detector: $\mathcal{O}(100) \rightarrow \mathcal{O}(1000)$ (x40)
- reducing the cell size: $150\,\mu m \times 150\,\mu m \rightarrow 50\,\mu m \times 50\,\mu m \rightarrow 25\,\mu m \times 25\,\mu m$ (soon)
- reducing the diameter of the columns: $6 \sim 10\,\mu m \rightarrow 2.6\,\mu m \rightarrow 1 \sim 2\,\mu m$ (soon)
- $\rightarrow$ increasing column yield: $\sim 90\,\% \rightarrow \geq 99.8\,\%$
- recently tested first irradiated $50\,\mu m \times 50\,\mu m$ 3D detector $(3.5 \cdot 10^{15}\,n/cm^2)$

3D Pixel Detectors:

- visible improvements with each step reducing the cell size
- all worked as expected (to first order)

Section 3

Results

Detectors

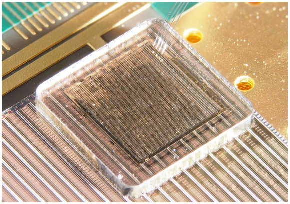

(a) B5

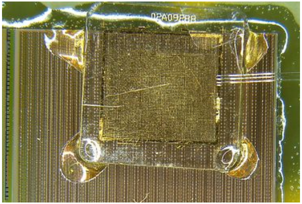

(b) B6

	B5	**B6**
readout chip (ROC)	FE-I4B	PSI46digv2.1respin
pixel pitch	250 µm × 50 µm	150 µm × 100 µm
3D cell size	50 µm × 50 µm	50 µm × 50 µm
ganging	5 × 1	3 × 2
size	4.90 mm × 4.94 mm	4.85 mm × 4.90 mm
thickness	510 µm	500 µm
50 pixels × 50 pixels	53 × 67	67 × 53
3D columns	7223	7223
column diameter	2.6 µm	2.6 µm
active area	3.2 mm × 3.5 mm	3.45 mm × 3.19 mm
bump bonding	tin silver (IFAE)	indium (Princeton)

II6-B5 - Efficiencies @ CERN

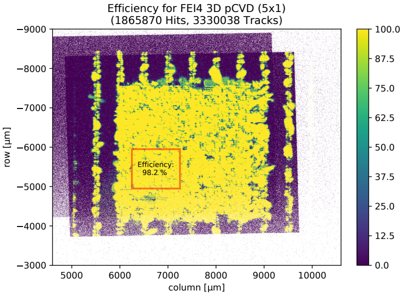

(a) Efficiency map.

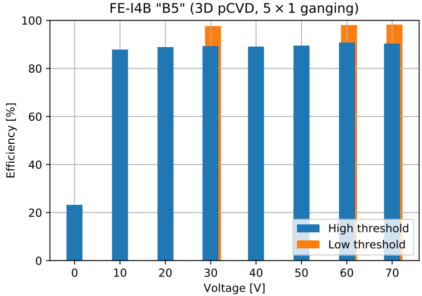

(b) Efficiency vs. bias voltage

- spatial resolution of $\sim$3 µm
- threshold of the chip: $\sim$1000 e
- efficiency in red fiducial area 98.2 %
- inefficiencies most likely due to bump bonding issues

Time Over Threshold

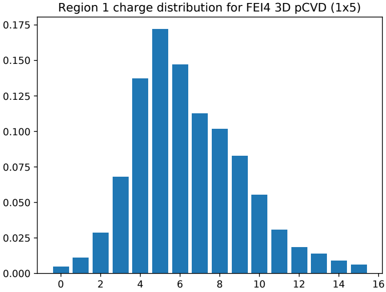

Figure: Time over threshold

- 5 tot $\approx$ 11 000 e
- mean of the ToT distribution: 6.7 $\rightarrow$ $\sim$15 000 e
- roughly 80 % the induced charge was collected

II6-B6 - Efficiencies @ PSI

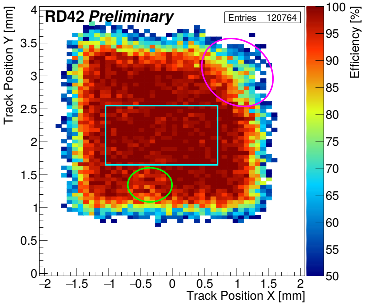

(a) Efficiency Map

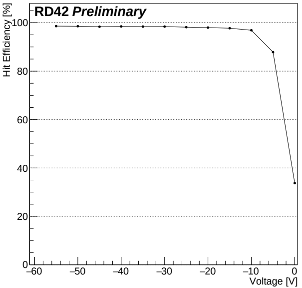

(b) Efficiency vs. voltage.

- spatial resolution of $\mathcal{O}\,(100\,\mu\text{m})$
- magenta area → bump bonding problems, green area → void in the diamond
- efficiency in blue box: 99.2 % (→ 0.4 % due to columns)
- already fully efficient at 30 V
- ROC stopped working after this beam test

Efficiencies @ CERN

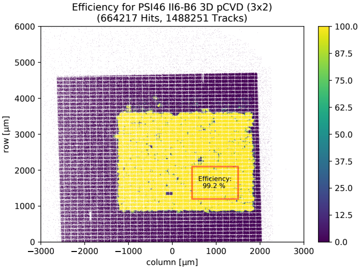

(a) Efficiency at threshold of ∼3500 e

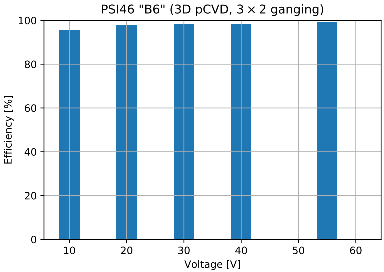

(b) Efficiency vs. bias voltage

- high resolution measurement at CERN
- find non-working/non-connected cells
- sensor twice re-bump-bonded with the same indium (no reprocessing)
  - no removal of old bumps, no change of surface metallisation
- same efficiency: 99.2 %

Pulse Height @ CERN

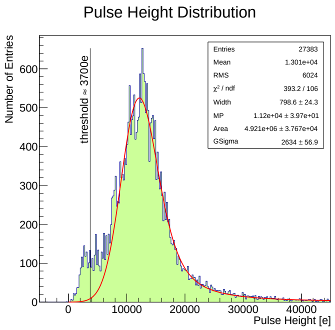

Figure: Pulse height distribution.

- threshold of the chip: ∼3700 e
- mean of the Langau fit: ∼15 000 e
- pulse height very similar to 5 × 1 result at CERN
- distribution below threshold not understood (maybe data transmission issues)

Section 4

Conclusion

Conclusion

- strongly improved fabrication of 3D diamonds
  - 40 times more cells
  - smaller cell size down to 50 μm × 50 μm
  - thinner columns down to 2 μm
- 3D Detectors work well in pCVD diamond
- general reasons for inefficiencies:
  - no charge created in the volume of the electrodes (0.4 % for shown devices)
  - region with low electric field
  - missing/broken columns
- 99.2 % efficiency in 3 × 2 ganged device
- 97.7 % efficiency in 5 × 1 ganged device
  - most likely processing issues
- consistent charge measurements for all devices: ∼11 000 e @ CERN SPS
- nearly full charge collection

Section 5

Outlook

Outlook

- analyse $3.5 \cdot 10^{15}\,\mathrm{n/cm^2}$ irradiated $50\,\mu\mathrm{m} \times 50\,\mu\mathrm{m}$ detectors
- test both $50\,\mu\mathrm{m} \times 50\,\mu\mathrm{m}$ and $25\,\mu\mathrm{m} \times 25\,\mu\mathrm{m}$ pixel detectors
- reduce column diameter to $1 \sim 2\,\mu\mathrm{m}$
- build pixel device on newest RD53 chip ($50\,\mu\mathrm{m} \times 50\,\mu\mathrm{m}$ pixel pitch)
- continue scale up by 10x

Del Fin